

# Advanced control and design methods of the auxiliary resonant commutated pole inverter

S. KARYŚ\*

Power Electronics Department, Kielce University of Technology, 7 1000-lecia P.P. Ave., 25-314 Kielce, Poland

**Abstract.** This paper presents several methods that enable the reduction of power loss in the auxiliary resonant commutated pole inverter – ARCP. Presented methods can be divided into static and dynamic ones. The static methods are related to an appropriate design of the inverter, whereas dynamic ones to advanced control of the power transistors. A variety of design and control methods are presented together with their advantages and disadvantages. The new control method of the current in the resonant branch is described. The main benefits of the proposed extended control method and their constrains are shown.

**Key words:** soft switching, ARCP, ZVS.

## 1. Introduction

The concept of the ARCP inverter was proposed by R. W. De Doncker in 1990 [1] but the basis was given by W. McMurray [2, 3] much earlier. The basic type of three phase inverter is shown in Fig. 1. In each phase the characteristic auxiliary branch can be seen. It consists of bi-directional switch (built from:  $T_a$  transistors and  $D_a$  diodes) and resonant inductor  $L$ . Resonant capacitors  $C_R$  are connected in parallel to each of the main transistors  $T$  switched on and off in zero voltage condition. The auxiliary transistors  $T_a$  are switching in zero-current conditions. The operational principles are extensively presented in the literature [1]. The ARCP type inverters for nominal power bigger than 20 kilowatts have conspicuously high efficiency (about 96%). The main fields of application of this type of inverter are: supply system for railway rolling stock, and the drive of electric and hybrid car.

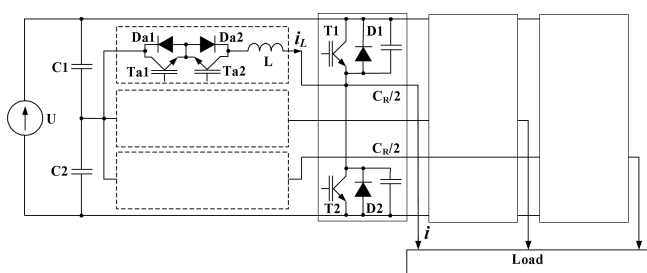


Fig. 1. Basic type of the three-phase ARCP inverter

From 1990 up to now, several ARCP type inverters have been invented. The classification of the power loss reduction methods is shown in Fig. 2. Figure 3 shows inductor current  $i_L$  during turn on and turn off process of the transistor T1. Two types of inductor current regions can be distinguished in Fig. 3. These are resonant and linear currents. The first one depends only on  $L$ ,  $C_R$  value (static method-design of the

resonant tank elements) while the second can be regulated by control system (dynamic methods).

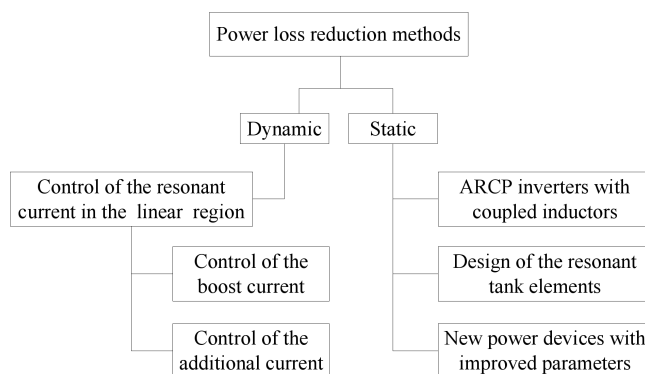


Fig. 2. Classification of the power loss reduction methods for the ARCP type inverters

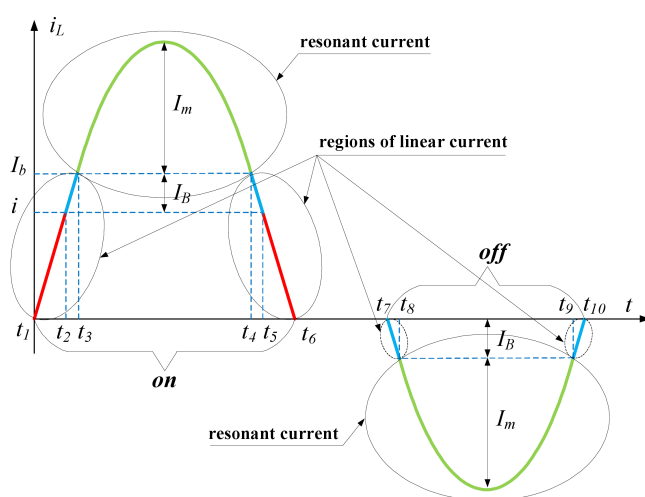


Fig. 3. Inductor current  $i_L$  at turn on and turn off process of the transistor T1

\*e-mail: enesk@tu.kielce.pl

## 2. Static power loss reduction methods

**2.1. ARCP inverter with coupled inductors.** Decreasing the rms value of the inductor current  $i_L$  by means of coupled inductors is the first static method that enables to reduce power loss in this type of inverter. Current  $i_L$  can be divided (usually by two) in the auxiliary circuit by means of coupled inductors. Figure 4 shows different phase diagrams of the ARCP inverter with coupled inductors where the resultant dissipation inductance of the transformer acts as the resonant inductance  $L$ .

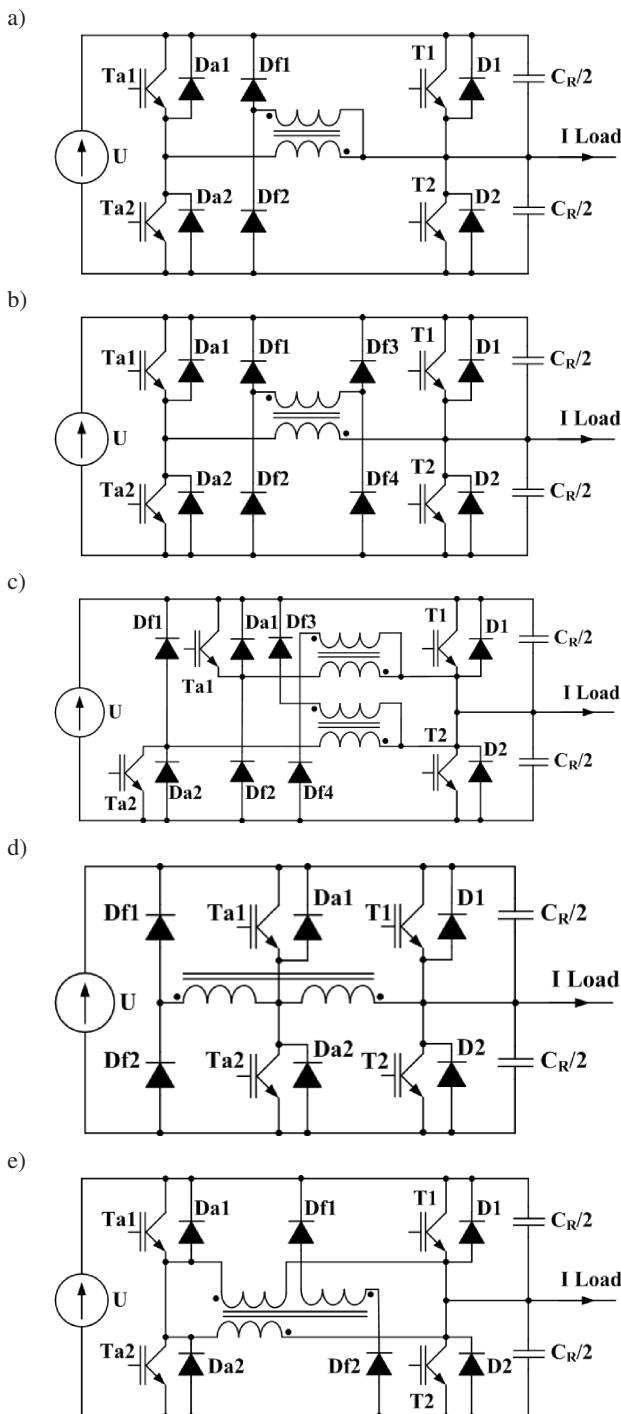


Fig. 4. Different types of the ARCP inverter with coupled inductors

The most popular type of the ARCP inverter with coupled inductors is shown in Fig. 4a [4, 5]. Typical turn ratio of the transformer is 1:1 and therefore, inductor current  $i_L$  in the auxiliary devices is divided by two. The main disadvantage of this solution and configuration shown in Fig. 4b [6] is overvoltage that appears when transformer current falls to zero. Saturated inductor added serially to transformer helps to discharge energy accumulated in its magnetic circuit and overvoltage is eliminated [7]. In comparison with a solution in Fig. 4a the inverter shown in Fig. 4c has two transformers. Inductor current  $i_L$  in the auxiliary devices is four times smaller which leads to the reduction of power loss in the auxiliary circuit and very high efficiency (98%) [8, 9]. The transformer shown in Fig. 4d provides full isolation and the problem of overvoltage does not appear [10, 11]. The modification shown in Fig. 4e [12] also eliminates overvoltage and has only two diodes. For this configuration the Tyco Electronics offers dedicated power module that enables constructing a 120kW three phase ARCP inverter.

The major advantage of the ARCP inverters with coupled inductors is the ability to reduce the resonant current. This directly causes power loss reduction in the auxiliary circuit. The mentioned problem of overvoltage can be easily solved. In most applications additional transformers weight and size are not considerable drawbacks. As for the time being the considered type of the ARCP inverter shows the best efficiency.

**2.2. Design of the resonant tank elements.** Two methods of the resonant tank elements design are described in literature. The first, proposed in [13, 14] emphasizes the possibility of using as large value of the resonant capacitor as possible. This disputable method leads to very small characteristic impedance  $Z$ . As a result, high amplitude of the resonant current  $I_m$  appears in Eq. (1).

$$I_m = \frac{U}{2Z} = \frac{U}{2\sqrt{\frac{L}{C_R}}}, \quad (1)$$

where  $U$  – amplitude of the supply voltage,  $L$ ,  $C_R$  – resonant inductor and capacitor respectively.

A high value of the current  $I_m$  increases all components of the total power loss in the ARCP resonant inverter.

A different approach is proposed in [15, 16]. The minimization of equation that describes resonant tank energy, gives minimal value of the resonant current amplitude  $I_m$

$$I_m = \frac{I_A}{1 + \sqrt{\pi/Q}}, \quad (2)$$

where  $I_A$  – amplitude of nominal load current,  $Q = \frac{Z}{R}$  – quality of the resonant circuit,  $R$  – total resistance of the resonant circuit.

Power loss in the auxiliary circuit is considerably reduced and values of resonant tank elements  $L$ ,  $C_R$  are called optimal. This ensures minimal value of energy oscillating in the resonant circuit.

It must be noticed that  $L, C_R$  are optimal for one contingency only, that is for instantaneous value of the load current  $i$  equal to  $I_A$ .

**2.3. New power devices with improved parameters** With regard to soft-switching operation of the main and auxiliary transistors in the ARCP inverter, the reduction of conduction power loss becomes the major goal. When the supply voltage is below 600 V, new generation of power MOSFET transistors shows an outstanding characteristics. For instance, STY139N65M5 transistor has only 14 mΩ static turn-on resistance and 650 V drain-source breakdown voltage. For the higher voltage range, the silicon-carbide technology offers more benefits. The most promising are SiC power MOSFET devices. They have simple control, low turn-on resistance (80 mΩ for 1200 V breakdown voltage), very good switching performance and high operating temperature capability (up to 300°C). The load current has strong influence on voltage drop in a different kind of power switches at turn-on stage. Nowadays the technique of matching power switches is often used. In [9] IGBT and power MOSFET transistors are connected in parallel. At low load current region, power MOSFET transistor conducts and when load current increases it flows through IGBT transistor. Therefore, this type of inverter has higher efficiency than a similar one built from one kind of power switches.

### 3. Dynamic power loss reduction method

The analysis of the basic type of the ARCP inverter shown in Fig. 5 is carried out for the following assumptions:

- the inverter is driven by ideal constant voltage source
- the transistor and diode are ideal switch with zero switching time
- the elements of the series-resonant circuit are passive, time-invariant, and do not have parasitic reactive components

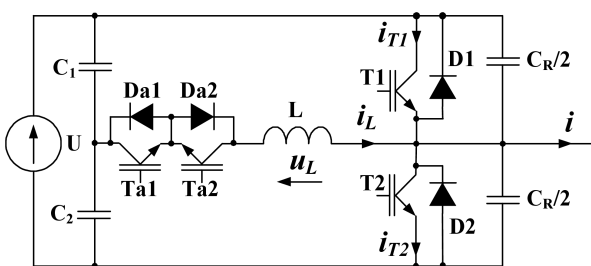


Fig. 5. Basic type of the ARCP inverter

From Fig. 6 it can be seen that inductor current  $i_L$  changes in linear manner at time periods:  $t_{1-3}, t_{4-6}$ , (turn on process) and  $t_{7-8}, t_{9-10}$  (turn off process).

Linear share of the current  $i_L$  at turn on process is equal to  $I_b = i + I_B$ . When the load current  $i$  has sinusoidal shape  $i = I_A \sin(\omega t)$  then  $I_b = I_A \sin(\omega t) + I_B$ . It means that the inductor current  $i_L$  ought to follow the load current and time period  $t_{1-2}$  is regulated according to equation:

$$t_{1-2} = \frac{2Li}{U} = \frac{2LI_A \sin(\omega t)}{U} \quad (3)$$

for  $\omega t \in \langle 0; \pi \rangle$ .

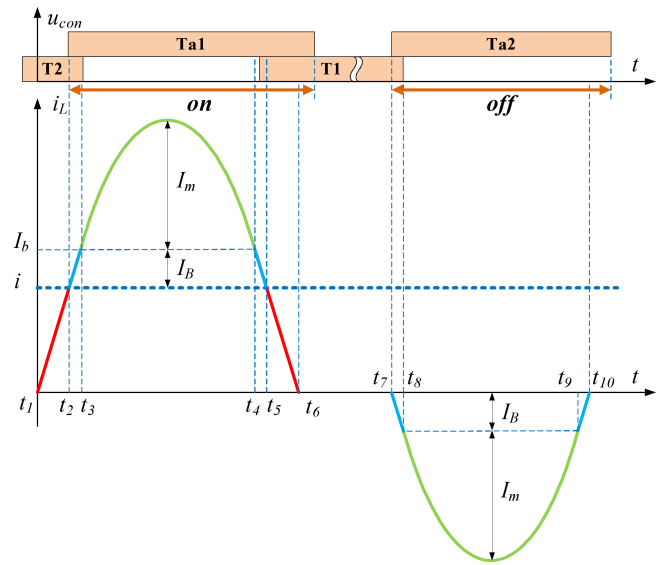


Fig. 6. Control signals and inductor current  $i_L$  for transistor T1 commutation, load current  $i > 0$

Time  $t_{2-3}$  period regulation is more complex. Additional current  $I_B = I_b - i$  is necessary to compensate the influence of resonant circuit resistance  $R$ . This current complements energy dissipated in the form of heat in a half of resonant period  $T_R/2$ . Thus the following inequality has to be fulfilled:

$$\frac{L}{2}(I_b^2 - i^2) \geq R \int_0^{T_R/2} [I_b + I_m \sin(\omega_o t)]^2 dt \quad (4)$$

after introducing  $I_b = I_B + i$ ,  $k = I_m/I_A$  the inequality (4) can be written as

$$(Q/2 - \pi)I_B^2 + (Qi - 2\pi i - 4kI_A)I_B - \pi i^2 - 4kiI_A - (\pi/2)k^2I_A^2 \geq 0 \quad (5)$$

because  $I_B \geq 0$ , inequality (5) has one solution under condition  $Q > 2\pi$

$$I_B \geq \frac{-Qi + 2\pi i + 4kI_A}{Q - 2\pi} + \frac{\sqrt{(Qi - 2\pi i - 4kI_A)^2 + (Q - 2\pi)(2\pi i^2 + 8kiI_A + \pi k^2 I_A^2)}}{Q - 2\pi} \quad (6)$$

Finally the time period  $t_{1-3}$  is derived as the

$$t_{1-3} = \frac{2L}{U}(i + I_B) = \frac{2L}{U}(I_A \sin(\omega t) + I_B) \quad (7)$$

The coefficient  $k$  depends on implemented design method of the resonant tank elements and quality factor  $Q$ . Typically  $k$  varies from 0.8 to 1.2. If  $i = I_A \sin(\omega t)$  for  $\omega t \in (0, \pi)$  and  $k = 1$  then minimal value of the current  $I_B$  can be shown in the form of plots for different  $Q$  values (Fig. 7).

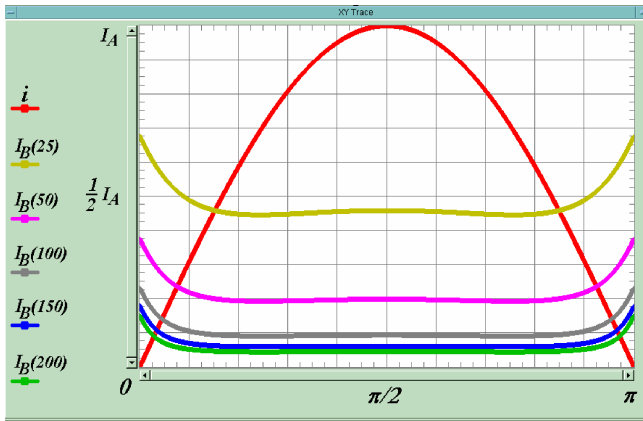


Fig. 7. Normalised load current  $i$  and current  $I_B(Q)$  for different quality factor  $Q$  values

From Fig. 7 it can be seen that current  $I_B$  has the maximum value when the load current  $i$  is equal to zero. Such a situation occurs at the time period  $t_{7-10}$  (a turn-off process Fig. 6). At the turn-on process, an additional current  $I_B$  has to be regulated in relation to an instantaneous value of the load current  $i$ . For  $Q \geq 100$  (racy case), current  $I_B$  decreases from about 20% ( $i = 0$ ) down to amount 10% of the  $I_A$  – nominal amplitude of the load current  $i$ . Advanced control techniques for ARCP type inverter presented in literature use a constant value of the current  $I_B$  (its value is once adjusted according to the  $I_A$ ). Due to current  $I_B$  regulation the instantaneous value of the inductor current  $i_L$  can be decreased which reduces power loss in the resonant circuit.

At time  $t_3$  (Fig. 6) current  $i_L$  is equal to  $i_b = i + I_B$ , the main transistor T2 is turned off and stage of current  $I_B$  forming is completed. In practice transistors timing parameters such as: turn-on and turn-off time (that depends on conduction current) have to be taken into account in control system. Additionally, if the parallel diode D2 reverse recovery time  $t_{rr}$  is greater than transistor T2 turn-on time, the time period  $t_{2-3}$  increases causing the increase of  $I_B$  current.

The transistor and diode timing characteristic influencing inductor current  $i_L$  can be compensated by modification of control signals time period in the function of the load current  $i$ .

#### 4. Experimental results

Figure 8 shows diagram of the research stage. The experimental basic type of the ARCPI inverter (structure shown in Fig. 1) is fed from three phase AC line through a bridge rectifier and  $L_{dc}$ ,  $C$  filter. An inverter has the following main design parameters:  $U = 538$  V, amplitude of nominal phase current  $I_A = 7$  A, resonant time period  $T_R = 3.8 \mu s$ ,  $L = 27 \mu H$ ,  $C_R = 13.5$  nF, switching frequency  $f_s = 10$  kHz. The HGTG5N120BND IGBT transistors were used as main and auxiliary power switches. The induction squirrel cage motor type Sb90-45, 230/400V, 5/2.9A, 50 Hz, 1380 obr/min, 1.1 kW was used as the load.

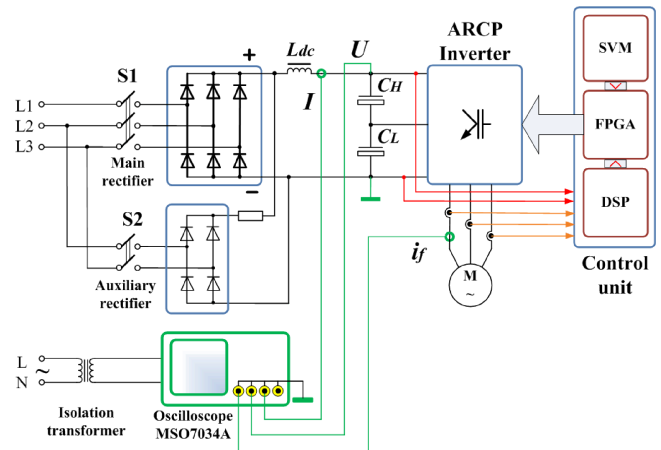


Fig. 8. Research stage diagram

Figure 9 shows experimental plots of the inductor current  $i_L$  and load current  $i$  in one phase of the induction motor. It can be noticed that inductor current  $i_L$  follows the load current  $i$ . The characteristic waveforms for main transistor at one cycle turn-off and turn-on processes are shown in Fig. 10. When observing collector current  $i_C$  and emitter-collector voltage  $u_{CE}$  it is seen that a zero-voltage switching condition is met.

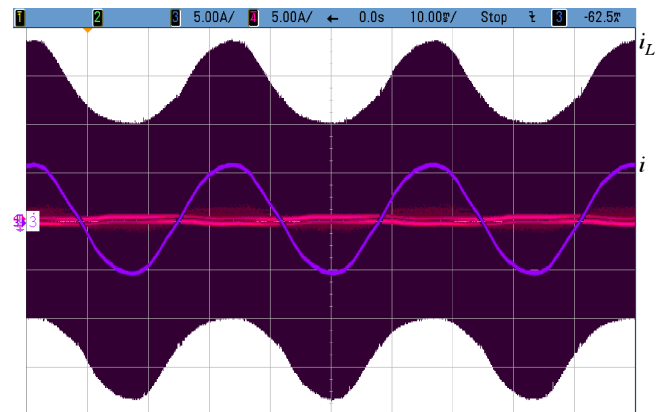


Fig. 9. Phase load current  $i$  and inductor current  $i_L$

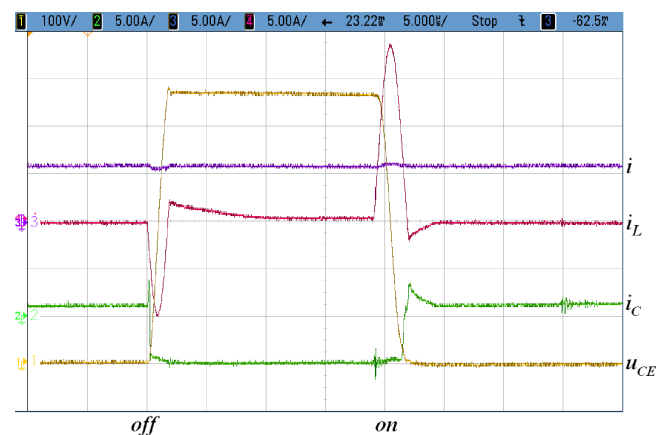


Fig. 10. Characteristic waveform at turn-off and turn-on processes:  $i$  – phase load current,  $i_L$  – inductor current,  $i_C$  – main transistor collector current,  $u_{CE}$  – collector-emitter voltage

To obtain current  $I_B$  regulation shown in Fig. 7, the control unit (FPGA module in Fig. 8) has to generate control signal with adequate time resolution.

It is assumed that half of the resonant period  $T_R/2 \cong 2 \mu\text{s}$  (typical case), the maximum time period  $t_{1-2}$ , when the inductor current  $i_L$  increases linearly from zero to  $I_A$ , reaches about  $0.7 \mu\text{s}$  (Fig. 10 turn-on process). As it was mentioned, for  $Q \geq 100$ , current  $I_B$  has to be regulated (by  $t_{2-3}$  time period changing) from about 20% down to 10% of the  $I_A$ . Therefore, the modification of control signals width is equal to  $\Delta t_{2-3} = (0.2 - 0.1)t_{2-3} \cong 70 \text{ ns}$  (in the analyzed case). The built experimental control system has 25ns resolution. An example of the  $I_B$  current approximation used in the control system ( $t_{1-2} = 0.7 \mu\text{s}$ ) is shown in Fig. 11.

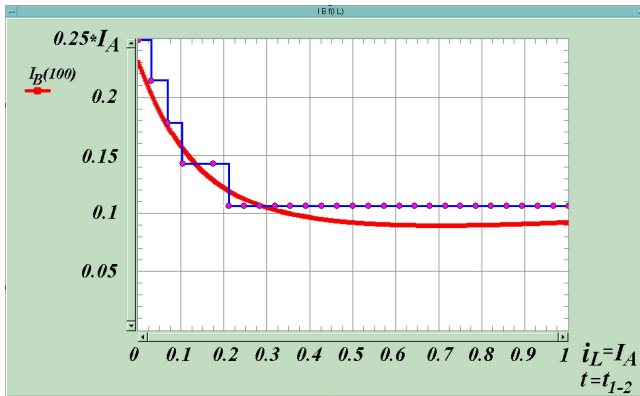


Fig. 11. Current  $I_B$  approximation in control system

When analyzing the plots in Fig. 11 it can be noticed that a control system should have higher resolution – about 10ns for better current  $I_B$  tracing.

The proposed current  $I_B$  regulation effect on power loss in the ARCP inverter is very difficult to measure because of its high efficiency. A high precision calorimetric measuring system shown in [8] is indispensable.

To estimate  $I_B$  regulation influence on power loss reduction, the mathematic loss model described in [17] was applied. The power loss computation was provided for the following conditions:  $U = 540 \text{ V}$ ,  $I_A = 7 \text{ A}$ ,  $f = 50 \text{ Hz}$ ,  $\cos \varphi = 0.85$ ,  $f_S = 10 \text{ kHz}$ ,  $T_R = 3.8 \mu\text{s}$ , amplitude factor  $A = 1$ ,  $Q = 100$ ,  $R_{ESR} = 0.1 \Omega$ , transistor and parallel diode voltage drop, switching energy loss were taken from HGTG5N120BND IGBT transistor data sheet.

Figure 12 shows the power loss averaged for a modulation period in: equivalent serial resistance ( $P_{esr}$ ) and conduction power loss ( $P_{ca}$ ). These components of the total power loss  $P_{tot}$  depend on current  $I_B$  and were calculated for half of the load current period – 10 ms.

From Fig. 12 it is seen, that  $I_B$  regulation gives distinct power loss reduction in the auxiliary circuit. Table 1 shows average power loss calculated from Figs. 12 and 13.

Mathematical calculations show that in the analyzed case proposed  $I_B$  regulation makes it possible to reduce total power loss by 3.8% in comparison with a control method, with a constant current  $I_B$  value.

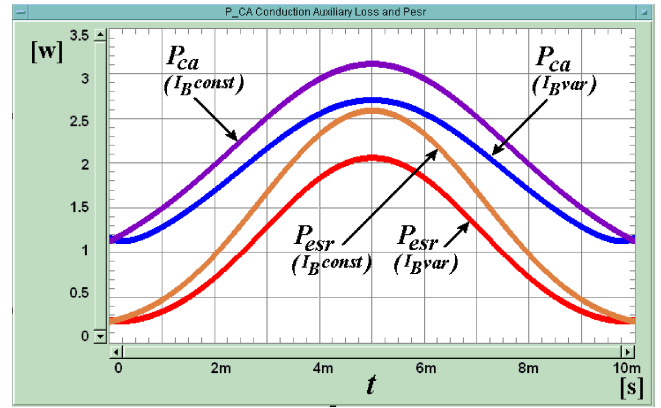


Fig. 12. ESR ( $P_{esr}$ ) and conduction power loss ( $P_{ca}$ ) in the auxiliary circuit for constant (const) and regulated (var) current  $I_B$

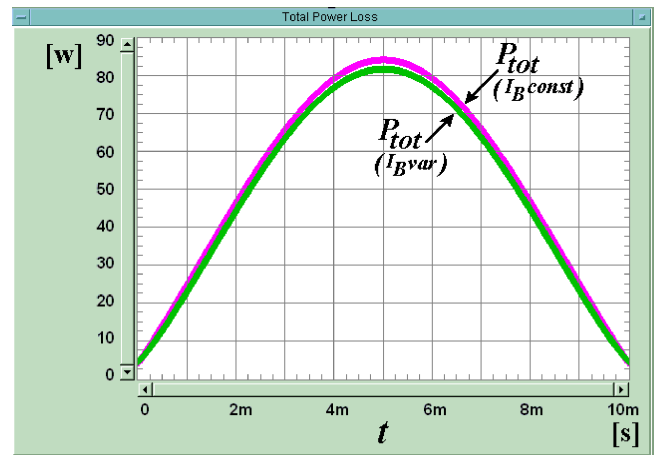


Fig. 13. Total power loss ( $P_{tot}$ ) for constant (const) and regulated (var) current  $I_B$

Table 1  
Average power loss

Average power loss W	Control method		Loss reduction %
	$I_B$ const	$I_B$ var	$\frac{P_{I_B const} - P_{I_B var}}{P_{I_B const}}$
Conduction $P_{ca}$	2.220	1.928	13.2
ESR $P_{esr}$	1.378	1.070	13.0
Total $P_{tot}$	52.6	50.6	3.8

## 5. Conclusions

A variety of methods causing higher efficiency of the ARCP inverter have been discussed in this paper. In particular, control of the additional inductor current  $I_B$  in the function of the load current  $i$  was presented. This technique has considerable potential for power loss reduction in the auxiliary circuit, since power loss in the serial resistance of the resonant circuit (ESR) depends on the square of rms value of the inductor current  $i_L$ . Decreasing current  $I_B$  by about 10% with regard to amplitude of the load current  $I_A$  is a considerable attainment. Experimental results show that in order to obtain current  $I_B$  regulation the control system is characterized by a high pulse with resolution of 10ns or higher. Nowadays, FPGA based

control unit enables reaching the required resolution and assigning new control standards.

## REFERENCES

- [1] R.W. De Doncker and J.P. Lyons, "The auxiliary resonant commutated pole converter", *Proc. IEEE-IAS* 1, 1228–1235 (1990).
- [2] W. McMurray, "SRC inverter commutated by auxiliary impulse", *IEEE Trans. Communications and Electronics* 8–75, 824–829 (1964).
- [3] W. McMurray, "Resonant snubbers with auxiliary switches", *Proc. IEEE-IAS* 1, 829–834 (1989).
- [4] S.C. Frame, D. Katsis, D.H. Lee D. Boroyevich, and F.C. Lee, "A three-phase zero-voltage-commutation inverter with inductor feedback", *Proc. IEEE-PESC* 1, 4708–4716 (1997).
- [5] C. Inaba, T. Yamazaki, M. Yoshida, E. Hiraki, Y. Konishi, and M. Nakaoka, "Three phase soft switching inverter with pulse current transformer - assisted resonant snubbers", *Proc. IEEE-ISIE* 1, 1106–1111 (2000).
- [6] I. Barbi and D.C. Martins, "A true PWM zero-voltage switching pole with very low additional rms current stress", *Proc. IEEE-PESC* 1, 261–267 (1991).
- [7] S. Karyś, "Three-phase soft-switching inverter with coupled inductors experimental results", *Bull. Pol. Ac.: Tech.* 59 (4), 535–540 (2011).
- [8] P. Sun, J.S. Lai, H. Qian, W. Yu, C. Smith, and J. Bates, "High efficiency three-phase soft-switching inverter for electric vehicle drives", *Proc. IEEE Vehicle Power and Propulsion Conf.* 1, 761–766 (2009).
- [9] P. Sun, J.S. Lai, H. Qian, W. Yu, C. Smith, J. Bates, B. Arnet, A. Litvinov, and S. Leslie, "Efficiency evaluation of a 55kW soft-switching module based inverter for high temperature hybrid electric vehicle drives application", *Proc. Applied Power Electronics Conf. and Exposition (APEC), Twenty-Fifth Annual IEEE* 1, 474–479 (2010).
- [10] X. Yuan and I. Barbi, "A transformer assisted zero voltage switching scheme for neutral-point-clamped (NPC) inverter", *Proc. IEEE-APEC* 1, 1259–1265 (1999).
- [11] X. Yuan and I. Barbi, "Analysis, designing, and experimentation of a transformer-assisted PWM zero-voltage switching pole inverter", *IEEE Trans. on Power Electronics* 15, 72–82 (2000).
- [12] P. Sontheimer and A. Mathoy, "Power for automotive and hybrid electric vehicle applications", *Power Systems Design Europe* 14–20, CD-ROM (2006).
- [13] W. Dong, J. Choi, H. Yu, F.C. Lee, "A 50 kW auxiliary resonant commutated pole inverter for electric vehicle applications-practical issues", *Proc. IEEE-PESC Conf. Rec.* 1, 136–141 (2001).
- [14] W. Dong, J. Choi, H. Yu, F.C. Lee, D. Boroyevich, and J. Lai, "Comprehensive evaluation of auxiliary resonant commutated pole inverter for electric vehicle applications", *Proc. IEEE-PESC* 1, 625–630 (2001).
- [15] J. Dawidziuk, *Power Loss Analysis in the Pole Commutated Voltage Source Feed Inverters*, Publishing Department of Bialystok University of Technology, Bialystok 2002, (in Polish).
- [16] S. Karyś, "Selection of resonant circuit elements for the AR-CP inverter", *Proc. IEEE-10th Int. Conf. on Electrical Power Quality and Utilisation* 15–17, CD-ROM (2009).
- [17] S. Karyś, "Power loss comparison for the arcp resonant inverter regard to control method", *Przegląd Elektro-Techniczny* 11, 64–68 (2008).